Interpolation Artefacts in Non-rigid Registration

P. Aljabar[1], J.V. Hajnal[2], R.G. Boyes[3], and D. Rueckert[1,⋆]

[1] Department of Computing, Imperial College London, U.K
[2] Robert Steiner MRI Unit, Imaging Sciences Department, Clinical Sciences Centre, Hammersmith Hospital Campus, Imperial College London, U.K
[3] Dementia Research Group, Institute of Neurology, University College London, U.K

Abstract. Voxel based non-rigid registration of images involves finding a similarity maximising transformation that deforms a source image to the coordinate system of a target image. In order to do this, interpolation is required to estimate the source intensity values corresponding to transformed target voxels. These interpolated source intensities are used when calculating the similarity measure being optimised. In this work, we compare the extent and nature of artefactual displacements produced by voxel based non-rigid registration techniques for different interpolators and investigate their relationship to image noise and global transformation error. A per-voxel similarity gradient is calculated and the resulting vector field is used to characterise registration artefacts for each interpolator. Finally, we show that the resulting registration artefacts can generate spurious volume changes for image pairs with no expected volume change.

1 Introduction

A common step in medical image processing is the application of voxel based registration techniques to 3D image volumes. Non-rigid registration is increasingly used to produce displacement fields that, with the emergence of deformation based morphometry [1] [6], have been used to provide data for further analysis. For example, the transformations estimated by registration can be used to generate Jacobian determinant maps in order to estimate volume changes [2] [6] [9]. Clearly, errors during non-rigid registration can lead to artefacts in the resulting transformations or in subsequent data. This implies a need to characterise the extent and nature of such artefactual displacement.

When registering images, interpolation of intensities at non-grid locations plays a part in the generation of artefacts and this has been the subject of a variety of previous studies [11] [21] [10] [7] [13] [23] [15]. It is possible, for example, to study interpolators in spectral terms in order to determine how close they are to the ideal low pass filter [11]. Generalised interpolation is described in [21]

⋆ The authors would like to thank Dr Nick Fox and the Dementia Research Centre for their aid in this study.

J. Duncan and G. Gerig (Eds.): MICCAI 2005, LNCS 3750, pp. 247–254, 2005.

where interpolators are assessed using approximation theory and according to performance. A review of the literature on interpolator performance in various image processing tasks is given in [10] where the kernels and spectral properties are described. In the context of registration, interpolators have been been studied in a variety of ways. It is possible to assesses interpolators for artefacts by identifying local optima in the similarity metric under known misregistrations [23]. The effect of grid alignment under misregistration on joint histogram dispersion is investigated in [15] to demonstrate how optima in the similarity metric can be created (linear and partial volume interpolation). Mutual information in particular has been shown [12] to be less susceptible to false local optima using partial volume interpolation in comparison with linear and nearest neighbour interpolation during rigid registration.

Previous work on registration artefacts has, as far as we are aware, focused on rigid and affine transformations where local optima in the similarity metric are identified as a single affine parameter varies. Non-rigid registration, however, can generate small localised displacements suggesting an increased chance of artefact. An example could be a sharp contrast boundary, blurred by a linear interpolator, being sharpened by local (artefactual) contraction. In this paper we characterise interpolation artefacts in non-rigid registration. We show that the gradient of the similarity metric can be used to indicate the degree of artefacts. We have also assessed the effects of noise and global registration error in non-rigid registration. Finally, using repeat MR scans for 11 subjects, we demonstrate that non-rigid registration can generate spurious volume change where they are not expected.

2 Methods

Theoretically, registering an image pair created by sampling the same underlying continuous signal at different locations should produce no displacement. This can only occur if the constraints of the sampling theorem are met and the interpolator used has ideal spectral properties (uniformly one in pass-band and zero elsewhere). Thus, the departure of the registration from the ideal behaviour (zero displacement) can be used to measure the extent of interpolation artefacts. In most non-rigid registration algorithms the course of the registration is determined by the gradient of the similarity metric. Thus, the gradient of the similarity metric provides an alternative measure to characterise interpolation artefacts. In particular, this measure is independent of the particularities of any non-rigid registration algorithm such as the representation of the displacement field. In this paper the similarity metric investigated is the sum of squared differences (SSD).

Similarity Gradient. Many non-rigid registration algorithms rely on the minimization of a similarity measure like sums of squared differences using gradient descent techniques [4] [22] [14]. Let S and T be the images to be registered such that S is the interpolated source image and T is the target image. For a current transformation estimate f, from T to S, the SSD is calculated using a set of grid locations x_i in image T and their transformed locations $f(x_i)$ in image S.

$$SSD = \frac{1}{n}\sum_{i=1}^{n}(S(f(x_i)) - T(x_i))^2$$

where the $S(f(x_i))$ and $T(x_i)$ represent the intensities at the corresponding locations in S and T. Generally, $S(f(x_i))$ represents an interpolated intensity. The chain rule can be used to derive the SSD gradient with respect to displacements of individual voxels

$$\nabla SSD = \frac{\partial(SSD)}{\partial S}\nabla S|_{f(x_k)} = \frac{2}{n}(S(f(x_k)) - T(x_k))\nabla S|_{f(x_k)} \quad (1)$$

The estimate for the source image gradient $\nabla S|_{f(x_k)}$ is obtained using central differences from the transformed source image $S(f(x_i))$.

Interpolators. In this paper we investigated four different interpolators: Linear, piece-wise continuous cubic (PCC) spline [8,16], cardinal spline (based on a cubic B-Spline kernel) [24] and a sinc-based interpolator that was apodised using a width 12 Hanning window and was renormalised [20].

3 Results

We have used simulated and real data to assess non-rigid registration artefacts. In addition we have used data from a routine clinical study to assess non-rigid registration artefacts by estimation of global volume changes.

Simulated Data. For our simulations we used a 2D slice from the Montréal Neurological Institute (MNI) simulated MR image [5] to create a second image with sample locations offset by half a pixel in the x direction. This was done by applying a linear phase shift to the Fourier spectrum of the original image so that, as far as possible, both images have the same spectral content. Using the global transformation of a half voxel shift along the x axis and each of the interpolators, the SSD gradient field was calculated for the simulated image pair. The magnitudes of the field are shown in figure 1 as a cumulative frequency curves for each interpolator. If the cumulative frequencies for an interpolator reach high percentiles quickly, the SSD gradient magnitudes tend to be low indicating a low artefact potential. Figure 1 shows a clear order for the interpolators from best to worst as : sinc, cardinal, PCC then linear.

For comparison, the images were registered using a non-rigid registration algorithm [17]. The magnitudes of the resulting displacements are shown as cumulative frequencies in the left of figure 1. The clear separation of the interpolators is preserved and their order matches that shown by the SSD gradient. However, the cumulative frequency curves for the displacements appear smoothed relative to those for the SSD gradient, something that can be explained by the intrinsic smoothness of displacement fields represented by B-splines [17].

Separate experiments were conducted to determine the robustness of the relative ordering of the interpolators with respect to noise. The order of the interpolators remained stable until high SNR values are reached (≈ 12). Beyond

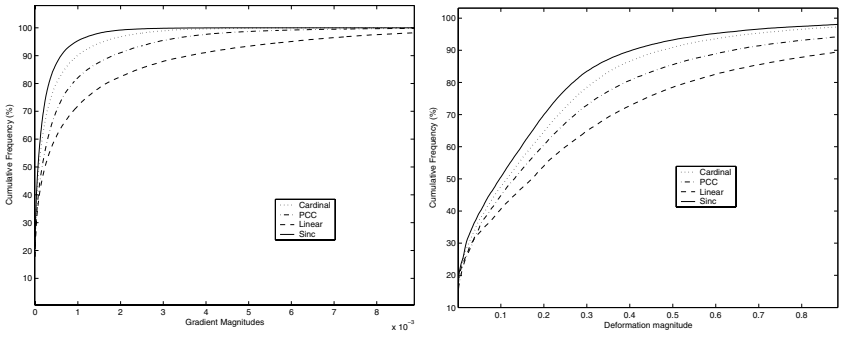

Fig. 1. Left: Cumulative frequency curves showing the distribution of magnitudes for the SSD gradient fields evaluated from the simulated MR image pair using each of the interpolators. Right: Cumulative frequency curves for the displacement fields obtained by registering the same images.

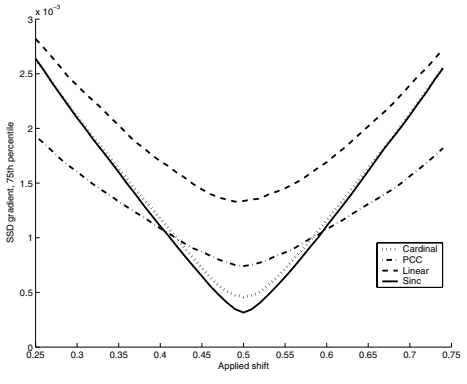

Fig. 2. A graph to show the effect of global registration error on the 75th percentile of the SSD gradient field. The horizontal axis shows the shift used as the global transformation estimate when calculating the SSD gradient. A shift of 0.5 voxels represents the 'true' transformation.

this point the linear interpolator performs best, something that can be explained by the relatively high degree of blurring it performs.

The effect of global misregistration was tested by varying the transformation estimate in equation (1). The size of the SSD gradient field, represented by its 75th percentile, is plotted against the applied shift in figure 2 where, for example, it can be seen that at an applied shift of 0.6, an error in the global transformation of a tenth of a voxel, there is little to distinguish the sinc, PCC and cardinal interpolators.

Real Data. To assess non-rigid registration artefacts in real data, two T1 weighted volumes were used that were acquired from a single subject on the same day. They were acquired on a 3T Intera system (Philips Medical Systems,

Best, The Netherlands) using an MP-RAGE sequence with an acquired resolution of $0.937 \times 1.15 \times 1.2mm^3$ reconstructed to $0.9375 \times 0.9375 \times 1.2mm^3$ voxels. A single rigid registration was carried out using a linear interpolator to obtain an estimate for the global transformation prior to calculating the SSD gradient field.

Each of the grids for the real images, after global transformation, varies in its alignment relative to the other. This contrasts with the simulated images for which the relative grid alignment is uniform at all locations. Because the differences between interpolators are clearer where the image grids are misaligned, an 'interpolation map' was created showing the distance from each globally transformed target voxel to the nearest source voxel. High values in the interpolation map indicate regions where the interpolation plays a more significant role.

The statistics of the SSD gradient were calculated where the brain region intersected the interpolation map thresholded at 75%. Figure 3 shows part of the resulting cumulative frequencies. Again, this correlates very well with the displacements generated from a non-rigid registration of the volumes (figure 3, right). The order of performance of the interpolators is well preserved. In both cases, the sinc and cardinal interpolators are however hard to distinguish, although both of these perform better than the PCC interpolator which in turn out-performs the linear interpolator.

Clinical Data. A common clinical application of non-rigid registration that could be affected by artefacts is the identification of volume differences between two sets of images. Recently, the use of transformations and their Jacobian determinants has been a useful tool in such volumetric approaches [2] [6] [9]. To test the effect of artefacts on volume change estimation a separate experiment was carried out using images from 11 subjects. All subjects were scanned twice on the same day using a 1.5T Signa Unit (GE Medical Systems, Milwaukee) with an IR-prepared spoiled GRASS sequence (TE, 6.4ms; TI, 650ms; TR 3000ms; Bandwidth 16KHz; 256x256x124 matrix; 240x240x186-mm FOV). Non-uniformity was corrected using N3 [19].

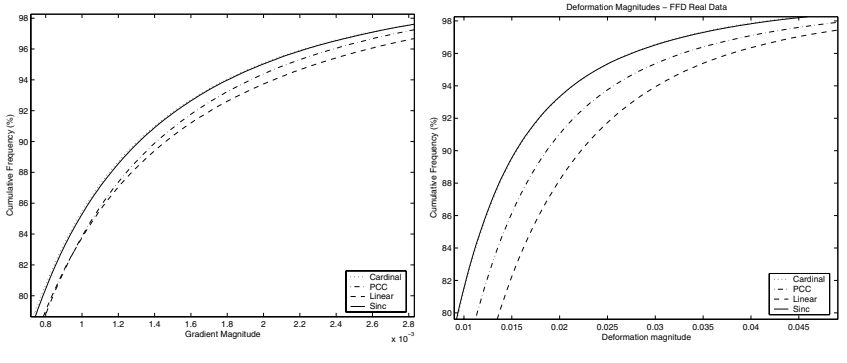

Fig. 3. Left: Cumulative frequency curves for the SSD gradient magnitudes derived using 2 acquired volumetric images. Each curve corresponding to a particular choice of interpolator. Right: The same curves for the displacement fields generated by registering the MR volumes.

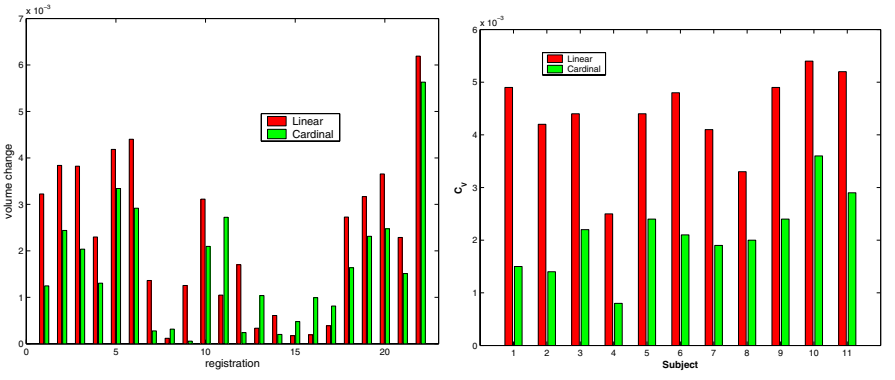

Fig. 4. Left: Volume changes generated by cardinal and linear based registrations for all 22 registrations (forward and reverse). Right: Volume consistency: Values of C_V calculated per subject for each of the linear (red) and cardinal (green) interpolators.

The departure of each registration from an expected zero volume change can be used to assess artefacts. The pairs were registered using the free-form deformation algorithm [17] in each direction producing 'forward' and 'reverse' transformations for both the linear and cardinal interpolators. The global volume change in the brain region was estimated for each transformation by integrating its Jacobian determinant (Figure 4 left). The mean volume changes were -0.22% and -0.11% for linear and cardinal interpolators respectively. A t-test showed this difference to be significant ($t = 12.5$, $p = 0.01$ gives critical value of $t = 2.5/2.8$ for 1/2 tailed tests). The volume changes were also highly correlated ($r^2 = 0.97$).

Given previous interest in registration consistency [18] [3], an estimate of volume change consistency was also calculated as a separate artefact measure. If D_{FR} represents the product of the forward and reverse volume changes then a measure of volume consistency C_V (symmetric for expansions and contractions) was defined as $C_V = |\log(D_{FR})|$. C_V should be zero for registrations that are truly volume consistent and higher values indicate increasing volume inconsistency. The values for all subjects are shown on the right of figure 4 which shows clearly better volume consistency for registrations using cardinal interpolation. Near identical results were obtained by evaluating the volume change directly from the composition of the forward and reverse transformations.

4 Discussion

In this paper we have shown how artefacts in non-rigid registration can be assessed using spectrally similar images the gradient of the similarity metric. Using SSD, the relative performance of different interpolators was assessed under 'ideal' conditions ('true' global transformation, zero noise) and under the effect of global misregistration and noise. This work has focused on interpolation artefacts in non-rigid registration while previous studies have concentrated on rigid and/or

affine registration. The relative performance of the interpolators as indicated by the SSD gradient compares favourably with that indicated by the results of registration. The metric investigated here was SSD although we recognise that other metrics can be more appropriate depending on the circumstances. If intensity based measures (e.g. canonical cross correlation) are used, for example with single modality images of the same subject acquired months apart, then the method presented can be readily extended. Information theoretic measures (e.g. Mutual Information) are often used for inter-modality registrations, in this case the definition of the similarity gradient (for example whether it has an analytic or numeric representation) will depend on how the measure is implemented. Registrations using an optimisation method other than first order gradient descent would require a modified version of an artefact estimator. For example, the Hessian should be a better estimator if second order descent is used.

In general, the results suggest that, for images with a reasonable noise level and a sufficiently accurate global registration step, there appears to be benefit in using more sophisticated interpolators (e.g. cardinal) over simpler ones (e.g. linear). The noise level also needs to be quite high before before interpolators become comparable in terms of artefact whereas a reasonably small global registration error can nullify the benefit of using a sophisticated interpolator. The results based on clinical data showed a significant difference between the volume changes generated by linear and cardinal interpolators. The high correlation of their volume changes indicates the degree to which image content determines artefactual effects. If the inter or intra-subject volume differences in a study are sufficiently small then the results can be affected by the choice of interpolator with the ability to discriminate groups better served by the use of a more sophisticated interpolator. Our results suggest that the use of the cardinal over the linear interpolator could mean a potentially shorter interval between scans in a longitudinal study or the use of fewer subjects in a cross-sectional study. Our results also show that registrations are more volume consistent using a cardinal interpolator compared to a linear interpolator.

References

1. J Ashburner, C Hutton, R Frackowiak, I Johnsrude, C Price, and K Friston. Identifying global anatomical differences: Deformation-based morphometry. *Human Brain Mapping*, 6(5):348–357, December 1998.
2. JP Boardman, K Bhatia, S Counsell, J Allsop, O Kapellou, Rutherford MA, AD Edwards, JV Hajnal, and D Rueckert. An evaluation of deformation-based morphometry in the developing human brain and detection of volumetric changes associated with pre-term birth. *MICCAI*, 2878:697–704, November 2003.
3. GE Christensen and HJ Johnson. Consistent image registration. *IEEE Trans. Med. Imaging*, 20(7):568–582, 2001.
4. GE Christensen, RD Rabbit, and MI Miller. A deformable neuroanatomy textbook based on viscous fluid mechanics. *Information Sciences and Systems*, pages 211–216, March 1993.
5. C.A. Cocosco, V. Kollokian, R.K.-S. Kwan, and A.C. Evans. Brainweb: Online interface to a 3d MRI simulated brain database. *NeuroImage*, 5(4):425, May 1997.

6. C Gaser, I Nenadic, BR Buchsbaum, EA Hazlett, and MS Buchsbaum. Deformation-based morphometry and its relation to conventional volumetry of brain lateral ventricles in MRI. *Neuroimage*, 13(6):1140–5, June 2001.
7. JV Hajnal, N Saeed, EJ Soar, and et al. A registration and interpolation procedure for sub-voxel matching of serially acquired MR-images. *JCAT*, 19(2):289–296, Mar-Apr 1995.
8. RG Keys. Cubic convolution interpolation for digital image processing. *IEEE Trans. Acoustics, Speech, And Signal Processing*, 29(6):1153, December 1981.
9. M Kubicki, ME Shenton, DF Salisbury, Y Hirayasu, K Kasai, R Kikinis, FA Jolesz, and RW McCarley. Voxel-based morphometric analysis of gray matter in first episode schizophrenia. *Neuroimage*, 17(4):1711–9, December 2002.
10. TM Lehmann, C Gonner, and K Spitzer. Survey: interpolation methods in medical image processing. *IEEE Trans. Med. Imaging*, 18(11):1049–1075, November 1999.
11. E Maeland. On the comparison of interpolation methods. *IEEE Trans. Med. Imaging*, 7(3):213–217, September 1988.
12. F Maes, A Collignon, D Vandermeulen, G Marchal, and P Suetens. Multimodality image registration by maximization of mutual information. *IEEE Trans. Med. Imaging*, 16(2):187–198, April 1997.
13. JL Ostuni, AKS Santha, VS Mattay, and et al. Analysis of interpolation effects in the re-slicing of functional MR images. *JCAT*, 21(5):803–810, September 1997.
14. X Pennec, P Cachier, and N Ayache. Fast non-rigid matching by gradient descent: Study and improvements of the demons algorithm. Technical Report 3706, INRIA, June 1999.
15. JPW Pluim, JBA Maintz, and MA Viergever. Interpolation artefacts in mutual information-based image registration. *Computer Vision and Image Understanding*, 77(2):211–232, February 2000.
16. SE Reichenbach and F Geng. Two-dimensional cubic convolution. *IEEE Trans. Image Processing*, 12(8):857, August 2003.
17. D Rueckert, LI Sonoda, C Hayes, DLG Hill, MO Leach, and DJ Hawkes. Non-rigid registration using free-form deformations: Application to breast MR images. *IEEE Trans. Med. Imaging*, 18(8):712–721, August 1999.
18. Oskar M. Skrinjar and Hemant Tagare. Symmetric, transitive, geometric deformation and intensity variation invariant nonrigid image registration. *ISBI*, pages 920–923, 2004.
19. JG Sled, AP Zijdenbos, and AC Evans AC. A non-parametric method for automatic correction of intensity nonuniformity in MRI data. *IEEE Trans. Med. Imaging*, 17(1):87–97, February 1998.
20. NA Thacker, A Jackson, D Moriarty, and et al. Improved quality of re-sliced MR images using re-normalized sinc interpolation. *Journal of Magnetic Resonance Imaging*, 10(4):582–588, October 1999.
21. P Thévenaz, T Blu, and M Unser. Interpolation revisited. *IEEE Trans. Med. Imaging*, 19(7):739–758, July 2000.
22. JP Thirion. Image matching as a diffusion process: An analogy with maxwell's demons. *Medical Image Analysis*, 2(3):243–260, 1998.
23. J Tsao. Interpolation artifacts in multi-modality image registration based on maximization of mutual information. *IEEE Trans. Med. Imaging*, 22(7):854–864, July 2003.
24. M Unser. Splines : A perfect fit for signal and image processing. *IEEE Signal Processing Magazine*, pages 22–38, November 1999.